General Disclaimer

One or more of the Following Statements may affect this Document

- This document has been reproduced from the best copy furnished by the organizational source. It is being released in the interest of making available as much information as possible.

- This document may contain data, which exceeds the sheet parameters. It was furnished in this condition by the organizational source and is the best copy available.

- This document may contain tone-on-tone or color graphs, charts and/or pictures, which have been reproduced in black and white.

- This document is paginated as submitted by the original source.

- Portions of this document are not fully legible due to the historical nature of some of the material. However, it is the best reproduction available from the original submission.

NASA Contractor Report 168166

IMPROVED DESIGN OF SUBCRITICAL AND SUPERCRITICAL CASCADES USING COMPLEX CHARACTERISTICS AND BOUNDARY LAYER CORRECTION

Jose M. Sanz

Universities Space Research Association
Columbia, Maryland 21044

May 1983

Prepared for

NATIONAL AERONAUTICS AND SPACE ADMINISTRATION
Lewis Research Center
Under Contract NAS3-22531

IMPROVED DESIGN OF SUBCRITICAL AND SUPERCRITICAL CASCADES USING COMPLEX CHARACTERISTICS AND BOUNDARY LAYER CORRECTION.

Jose M. Sanz*
Universities Space Research Association
Columbia, Maryland 21044

1. INTRODUCTION

The method of complex characteristics and hodograph transformation for the design of shockless airfoils was introduced by Bauer, Garabedian and Korn and has been extended by the author to design supercritical cascades with high solidities and large inlet angles.This new capability was achieved, [1], by introducing a new conformal mapping of the hodograph domain onto an ellipse and expanding the solution in terms of Tchebycheff polynomials. A new computer code was developed based on this idea.

The design of two-dimensional inviscid subcritical and supercritical cascades has been widely accepted as a method to produce axial compressor and turbine blades. With this method a number of sections, spanning from hub to tip, can be designed independently of each other and according to the flow conditions required in the spanwise direction. Five of these 2-d sections are usually enough to design a blade with considerable three dimensional effects.
In this design procedure the basic 2-d code has to be able to handle high solidities, usually at the hub sections, and high stagger or inlet angles at the tip sections, especially in compressor rotors. Low maximum thickness-to-chord ratios are desirable for compressor blades. For turbine blades large turning angles exceeding one hundred degrees will not be unusual and thick blades will be, in general, required for cooling purposes. In this case, thick trailing edges will be necessary.

In the first two sections of the paper we review the method and report some improved new designs of compressor and turbine blades. A midspan propeller section is also shown. Although the primary purpose of the new code is the design of supercritical cascades, emphasis is made in the design of subcritical cascades because of the robustness of the code in this type of design as well as the low C.P.U. and overall time necessary to achieve a good design.

The next section describes the results obtained with the incorporation of a turbulent boundary layer computation to the inviscid design code. The lag-entrainment method of Green, Weeks and Brooman has been incorporated into the code. As the inverse design code uses an input surface pressure distribution, it is especially well suited for this coupling. An inviscid blade is first designed with the approximate required inlet angle and Mach number, turning and solidity. The turbulent boundary layer computation is then switched on, and by modification of the input pressure distribution the required design conditions are obtained, ensuring that no separation occurs.

The last section describes a cascade grid generator based on the same elliptic transformation that the author has introduced for the inverse hodograph method. A single conformal transformation suffices to map a cascade plane onto the computational domain. Open trailing edges can be handled with this transformation. A grid generated with this procedure is shown for the Korn airfoil.

2. REVIEW OF THE METHOD

A complete description of the complex characteristic design method can be found in [2], and the elliptic hodograph transformation and new code has been described in [1].We briefly review the design method. The basic idea is to construct by numerical integration an analytic solution to the potential flow equations finding, along with this solution, the body that corresponds to a prescribed surface pressure distribution. The equations of potential flow can be written in the hodograph complex characteristics form

$$\varphi_\xi = \tau_+ \psi_\xi \qquad \tau_\pm = \pm i \frac{\sqrt{1-M^2}}{\rho} \qquad (1)$$

$$\varphi_\eta = \tau_- \psi_\eta$$

where φ and ψ are the potential and stream fuctions, and M and ρ are the Mach number and density. The complex characteristics coordinates ξ and η are defined by means of the conformal transfomations

$$f(\xi) = \log h - i\theta \qquad \frac{dh}{h} = \sqrt{1-M^2}\,\frac{dq}{q}, \qquad (2)$$

$$\overline{f(\eta)} = \log h + i\theta$$

and where h and θ are the Chaplygin hodograph variables and q is the modulus of the velocity vector. The characteristic coordinate ξ, and similarly η, is defined in a circular ring $1 \le |\xi| \le R$, The conformal transformation

$$w = \frac{1}{2}\left(\xi + \frac{1}{\xi}\right), \quad 1 \le |\xi| \le R \qquad (3)$$

maps this circular ring onto an ellipse. Any analytic fuction on the ellipse can be expanded in the form.

$$f(w) = \sum_0^\infty c_n T_n(w) = c_0' + \sum_1^\infty c_n' \left(\xi^n + \frac{1}{\xi^n}\right) \qquad (4)$$

---

*Visiting Research Scientist at NASA Lewis Research Center, Cleveland, Ohio 44135.

where

$$T_n(w) = \frac{1}{2^n}\left(\xi^n + \frac{1}{\xi^n}\right), \quad n = 1, 2, \ldots \qquad (5)$$

are the Tchebicheff polynomials, [1].

Because equations (1) are linear in a hodograph domain, a complete set of solutions can be found by solving the characteristic initial value problem

$$\psi(\xi,0) = g(\xi) = \overline{\psi(0, \bar{\xi})} \qquad (6)$$

where the regular part of the characteristic initial value function g can be expanded in terms of the Tchebycheff polynomials. The coefficients of that expansion can be determined by imposing the boundary value problem.

$$R_e\{\psi(\xi,\bar{\xi})\} = 0 \qquad (7)$$

This C.I.V.P. can be solved when the mapping function f is known, as the coefficients $\tau_\pm$ depend implicitly on it. On the other hand, the mapping function f is determined by the Dirichlet problem

$$R_e\{f(\xi)\} = \log h^* \qquad (8)$$

where h^* is based on the prescribed input speed distribution. Problems (7) and (8) can be solved by means of an iterative process,[1], [2].

The use of complex characteristics allows extension of the computation to mixed flows.Although the equations are established in the four-dimensional space of two complex variables, the computation is carried out in a two-dimensional manifold, conformally transformed from a two-dimensional rectangular computational domain. The topology of this manifold is such that it avoids the sonic surface where the equations of the flow become ill-conditioned.

The computation is started at a subsonic point and is continued through the complex domain until it reaches the real supersonic region without intersecting the sonic surface. In the supersonic region it first reaches the body surface and then the sonic line. This technique avoids the inaccuraces that the ill conditioning of the equations near the sonic line could introduce. The elliptic transformation, by restricting the position of the upstream and downstream points of infinity to the foci of the ellipse, makes it possible to simplify the topology of these paths of integration. For purely subsonic flows the two dimensional manifold where the solution is carried out becomes the 'diagonal' of the four dimensional space, simplifying and reducing the computation.

3. SUBSONIC AND SUPERSONIC DESIGN

A wide variety of airfoils in cascade can now be designed with this inverse design procedure. The input to the design code can be separated in three parts. First we specify a surface speed distribution. By means of this input speed distribution we control the aerodynamic performance on the airfoil.

Second, three design parameters must be given. These parameters are the radius R of the outer circumference of the circular ring in the hodograph domain, which controls the solidity of the cascade; the angle Theta which locates the leading edge stagnation point, and thereby controls the stagger angle; and a Mach parameter controlling the inlet Mach number.

The third set of parameters, or numerical parameters, is concerned with the accuracy versus computational speed of the design process. The parameters are grid size for the subsonic or supersonic region, number of Fourier coefficients for the mapping function ,number of iterations and others.

To achieve a good design, one could proceed in the following way. An input speed distribution is prescribed that reflects the desired aerodynamic behavior. Then the three design parameters are determined. The parameter R, that controls the solidity, can be chosen with values that in practical terms, varies from 1.4 for a solidity of approximately 2 to a value of 2.5 for lower solidities of about 1. In the same manner we set the angle Theta for the leading edge stagnation point and the input Mach number.

A run can be made with this set of input parameters, and the design parameters changed successively until we obtain the inlet flow conditions and solidity. The advantage of the elliptic transformation is that changes in each of the three parameters have little effect on the flow variables that the two other perameters control. For instance, large changes in the parameter Theta have small effects on the solidity.

Once we have obtained the required solidity, inlet Mach number, and inlet air angle the input speed distribution is modified. This modification increases or decreases the lift, and thus the turning angle of the blade, by changing the area enclosed by the speed distribution. When the required turning has been achieved, and hence the exit flow conditions, the input speed distribution is used to tailor the body geometry. The maximun thickness of the airfoil, the leading edge curvature, and the trailing edge thickness can then be adjusted.

If all the numerical parameters are kept at their default values, a subcritical airfoil can be designed with as little as 30 seconds of C.P.U. time per run on the I.B.M. 370-3033 at the NASA Lewis Research Center. Subcritical designs can be obtained with as few as 15 runs, including the boundary layer correction. This makes the design of subcritical airfoils a very fast and reliable process.

For transonic designs the situation is more complicated. In the first place, we do not know if a shockfree solution exists in the region we are searching. The paths of integration, although automated not to intersect the sonic line, can reach a wrong branch of the analytic solution. Also, limit lines can appear in the supersonic region. The number of points in the computational domain is much larger, both because the integration paths are longer and because a finer grid is required, increasing the C.P.U. time considerably. The procedure for a transonic design would be to obtain first a subsonic blade with flow characteristics close to the design in question. Then, raising the input Mach number a supersonic region will be formed and the design parameters tuned to obtain the desired blade. In the final stages, a transonic run with a fine grid and a Richardson extrapolation in both the subsonic and supersonic regions takes about 5 minutes of C.P.U. time on the same I.B.M. 370-3033.

We describe in the rest of this section six airfoils designed with this procedure.The first one is a transonic airfoil fit for a midspan section of a modern propeller. An inlet Mach number of .83 was reached before the appearance of limiting lines. The maximum thickness to chord ratio of .059 is reached at about 45 per cent of the chord, which makes it an attractive design. Figure 1 shows a hodograph plane for this airfoil. In figure 2 can be seen the surface Mach number distribution obtained and the inviscid airfoil. Figure 3 shows the relative position of the airfoils in the cascade plane. A cubic spline has been passed through the airfoil after subtracting the computed displacement thickness.

The next airfoil, figures 4 and 5, represents a tip section for a compressor rotor. The inlet Mach number reached is 0.86. This airfoil shows a large supersonic region on the suction side and an incipient supersonic bubble on the pressure side. The thickness-to-chord ratio at the trailing edge after substracting the displacement thickness is .024. We show next a low speed rotor tip section with a high inlet air angle of 71 degrees, see figures 6 and 7.

The code has been used to design two turbine blade sections shown in figures 8 to 11. The first one is a subcritical section with a solidity of 1.77 (gap to-chord-ratio of 0.56). The surface speed distribution presents an accelerated profile on both sides of the blade. A small amount of diffusion is present in the last 30 percent of the suction side to obtain the correct trailing edge opening. This airfoil has been designed to form the midspan section of a cooled turbine rotor.

After this subcritical design, we show a transonic turbine blade section with half the solidity of the previous section. This, naturally, implies that one half of the blades should be needed for a turbine rotor with this section. In assessing this design we lost 20 per cent of the flow turning. Also, the diffusion on the suction side is now considerable greater.

The last example is a turning vane designed to operate at both zero incidence and at 45° of positive incidence, with the same exit flow angle in both modes of operation. Because of the blunt leading edge, large maximum thickness-to-chord ratio, and high solidity this blade is capable of turning the flow for the 45° of positive incidence operation mode.

4. BOUNDARY LAYER CORRECTION

A turbulent boundary layer computation has been incorporated into the inviscid inverse design code. We follow the lag-entrainment method as developed by Green, Weeks and Brooman in reference [3]. This method contains less empirical factors than the classic of Nash and McDonald. It solves three ordinary differential equations for three independent parameters, the momentum thickness, the shape factor and the entrainment coefficient, instead of one O.D.E. for the momentum thicknes as in Nash and McDonald.

These three O.D.E. can be written as

$$\frac{d\theta}{ds} = \frac{C_f}{2} - (H+2-M^2)\,\frac{\theta}{q_e}\,\frac{dq_e}{ds},$$

$$\theta\,\frac{d\bar{H}}{ds} = \frac{d\bar{H}}{dH_1}\left[C_E - H_1\left\{\frac{C_f}{2} - (H+1)\,\frac{\theta}{q_e}\,\frac{dq_e}{ds}\right.\right. \qquad (9)$$

$$\theta\,\frac{dC_E}{ds} = F\left[\frac{2.8}{H+H_1}\left\{C_{\tau_{EQ}}^{1/2} - \lambda\, C_\tau^{1/2}\right\}\right.$$

$$\left.\left. + \left(\frac{\theta}{q_e}\frac{dq_e}{ds}\right)_{EQ} - \frac{\theta}{q_e}\frac{dq_e}{ds}\left\{1 + f\,(M^2)\right\}\right]$$

where the three independent parameters θ, $\bar{H}$ and C_E are defined by

$$\theta = \int_0^{\infty} \frac{\rho q}{\rho_e q_e}\left(1 - \frac{q}{q_e}\right)dy$$

$$\bar{H} = \frac{1}{\theta}\int_0^{\infty} \frac{\rho}{\rho_e}\left(1 - \frac{q}{q_e}\right)dy \qquad (10)$$

$$C_E = \frac{1}{\rho_e q_e}\frac{d}{ds}\left(\int_0^{\infty} \rho q\, dy\right)$$

The suffix e refers to flow variables at the edge of the boundary layer. The two other shape parameters and the skin friction coefficient are defined by

$$H = \delta^*/\theta$$

$$H_1 = \frac{1}{\theta}\int_0^{\infty} \frac{\rho q}{\rho_e q_e}\,dy \qquad (11)$$

$$C_f = \frac{\tau_w}{\frac{1}{2}\rho_e q_e^2}$$

We refer to [3] for the definition and value of the others coefficients, which are function of the entrainment coefficient and the local free-stream magnitudes.

The transition point at which the computation of the boundary layer is started is left as an input parameter. Of the three initial values necessary to numerically solve the system of ordinary differential equations (9), only the initial momentum thickness is specified as an input parameter. The other two are computed by means of the equilibrium relations established in [3].

As described before, once an inviscid airfoil has been obtained, the turbulent boundary layer correction is switched on. The transition point is usually set at the point where the adverse pressure gradient starts. The Stratford criterion is followed to diffuse the flow from this point to the trailing edge. The Nash-McDonald separation parameter

$$SEP = -\frac{\theta}{q}\frac{dq}{ds} \qquad (12)$$

is used to predict separation. Separation is predicted when this parameter reaches a value of 0.004. Figures 14 to 19 shows the values of the parameter SEP for the six airfoils that we have discussed in this paper. An initial Reynolds number based on momentum thickness of 320 is assumed.

5. ELLIPTIC GRID GENERATION

The elliptic transformation introduced in [1] to map the hodograph plane onto an ellipse can also be used to transform a cascade of airfoils in the physical plane onto an ellipse. Let z be a point in the physical plane of a cascade, and w the elliptic variable introduced in section 2. The domain of the variable w is the ellipse onto which the conformal transformation (3) maps the circular ring $1 < |\xi| < R$. Consider the conformal transformation defined by

$$\frac{dz}{dw} = -\frac{(w_T - w)}{w^2 - 1}\, e^{\sum_0^n c_n T_n(w)}$$

with $$w = \frac{1}{2}\left(\xi + \frac{1}{\xi}\right), \quad 1 \le |\xi| \le R \qquad (13)$$

and where $T_n(w)$ are the Tchebicheff polynomials defined in section 2.

This single transformation allows to map a cascade of airfoils with open trailing edge, onto the interior of the ellipse. Th airfoil is mapped over the boundary and the trailing edge of the airfoil is transformed onto the point w_T. The upstream and downstream points of infinity are mapped onto the foci of the ellipse $w = \pm 1$. The angle at the trailing edge is given by $\varepsilon \cdot \pi$.

The transformation (13) can efficiently be performed using fast Fourier transform with a well known iteration procedure first described by Theordorsen and Garrick, Ives and Liutermoza and Bauer Garabedian and Korn. It will be enough to say here that the convergence of the iterative procedure is achieved by imposing, at each iteration, the trailing edge gap condition

$$dx + i\,dy = \pi i \left\{ (w_T + 1)\, e^{\sum_0^n c_n T_n(-1)} - (w_T - 1)\, e^{\sum_0^n c_n T_n(1)} \right\} \qquad (14)$$

where dx and dy are the trailing edge opening in the x and y direction.

The solidity is controlled by the parameter R and the stagger angle by the location of w_T. A Newton iteration automatically changes these two parameters to obtain the input solidity and stagger angle.

A grid generated with this transformation is shown in figure 20 for the Korn airfoil.

Because of the equivalence established before between the ellipse and the circular ring, this circular ring can be used in conjunction with this transformation in the computational domain to solve the potential flow equations in an analysis mode.

6. CONCLUSIONS

The new design code based on the method of complex charcteristics and elliptic hodograph transformation is an efficient method for the design of airfoils in cascade. In particular, the design of subcritical cascades of airfoils is a very fast, robust and versatile process. The inverse design code can be made to interact with a turbulent boundary layer calculation to obtain airfoils with no separated flows at the design condition. The elliptic conformal mapping can also be used to generate grids for airfoils in cascade with open traling edges.

REFERENCES

1. Sanz, J.; "Design of Supercritical Cascades with High Solidity", AIAA Paper 82-0954, June 1982.

2. Bauer, F., Garabedian, P. R. and Korn, D.; Supercritical Wing Section I, II, III, Springer-Verlag, Berlin, 1972, 1975, 1977.

3. Green, J. E., Weeks, D. J., and Brooman, W. F.; "Prediction of Turbulent Boundary Layers and Wakes in Compressible Flow by a Lag-Entrainment Method", ARC-R/M-3791, RAE-TR-72231, 1977.

4. Ives, D. C., and Liutermoza, J. F.; Analysis of Transonic Cascade Flow Using Conformal Mapping and Relaxation Techniques. AIAA Paper 76-370, July, 1976.

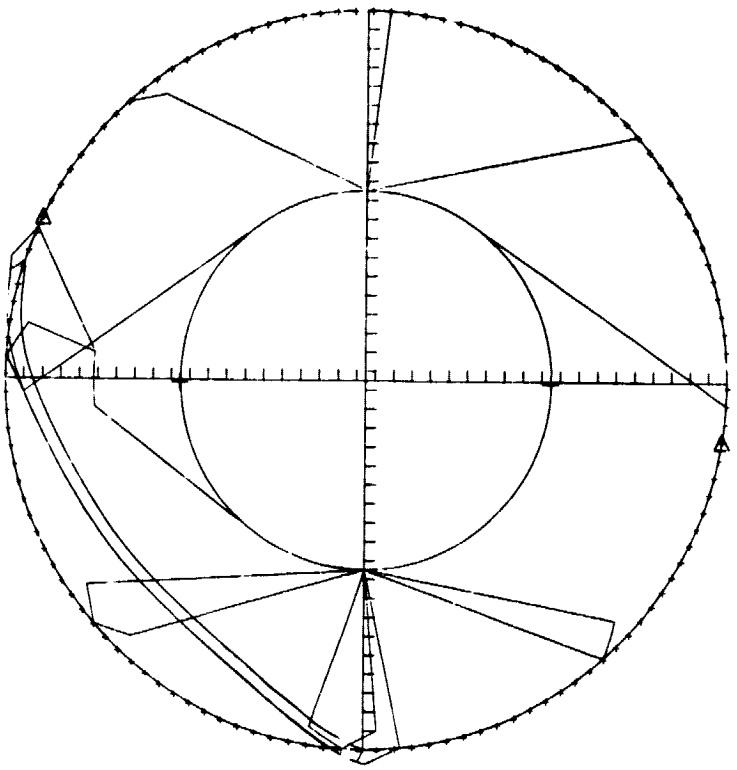

Figure 1. - Hodograph plane.

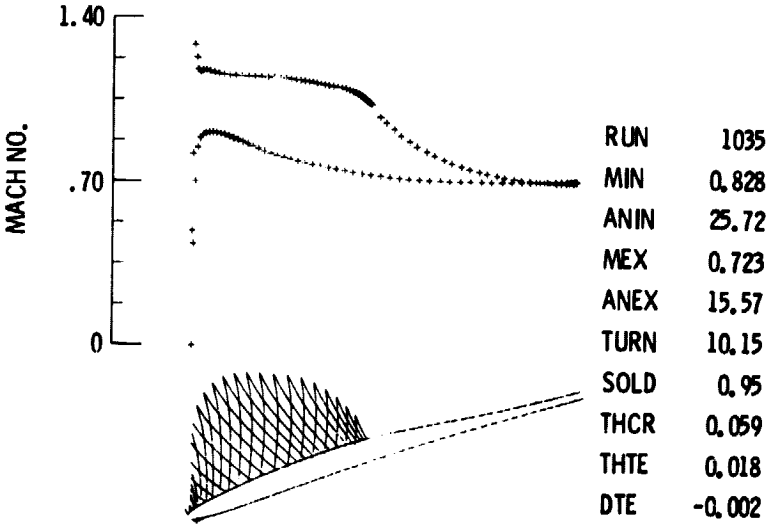

Figure 2. - Supercritical propeller section.

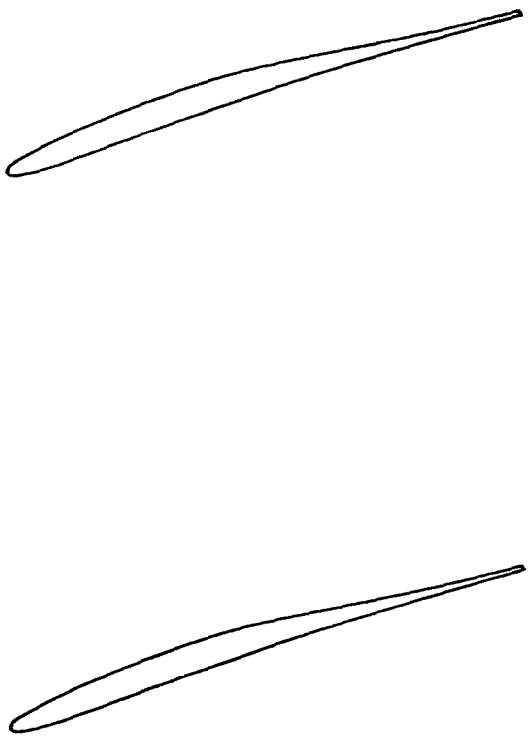

RUN	1035
RN	0.10E 07
MIN	0.828
ANIN	25.72
MEX	0.723
ANEX	15.57
TURN	10.15
SOLD	0.95
THCR	0.059
THTE	0.009
DTE	-0.002

Figure 3. - Supercritical propeller section.

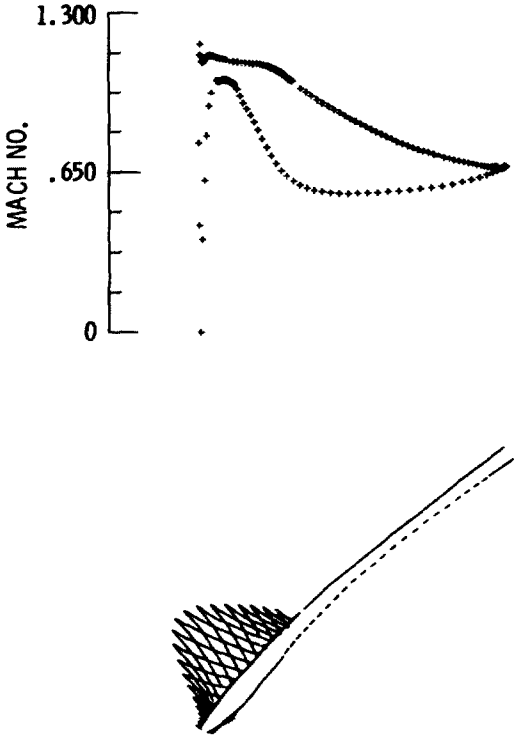

RUN	9004
MIN	0.864
ANIN	49.54
MEX	0.629
ANEX	38.82
TURN	10.72
SOLD	1.15
THCR	0.055
THTE	0.036
DTE	0.002

Figure 4. - Supercritical rotor section.

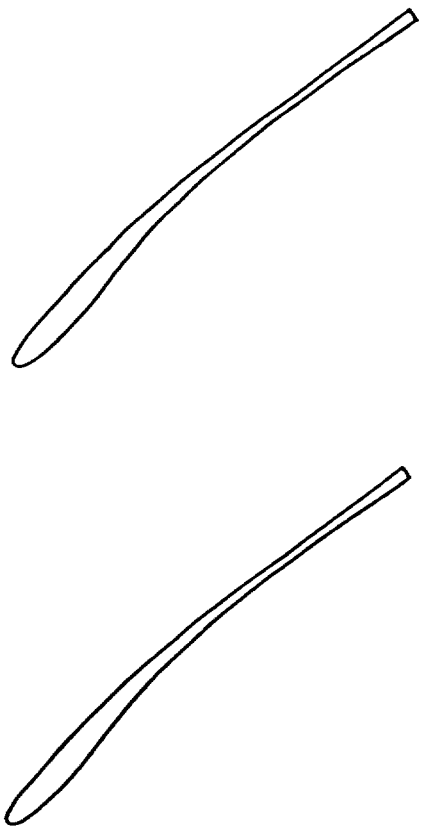

RUN	9004
RN	0.10E 07
MIN	0.864
ANIN	49.54
MEX	0.629
ANEX	38.82
TURN	10.72
SOLD	1.15
THCR	0.055
THTE	0.024
DTE	0.002

Figure 5. - Supercritical rotor section.

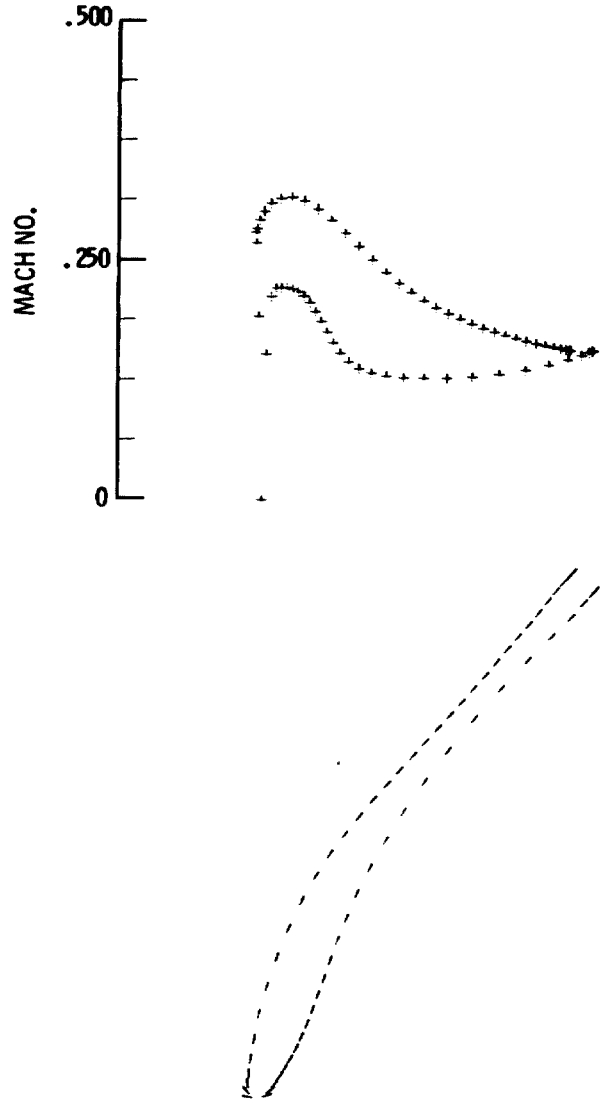

RUN	3069
MIN	0.259
ANIN	71.18
MEX	0.146
ANEX	51.80
TURN	19.37
SOLD	1.32
THCR	0.089
THTE	0.048
DTE	0.000

Figure 6. - High stagger subcritical rotor section.

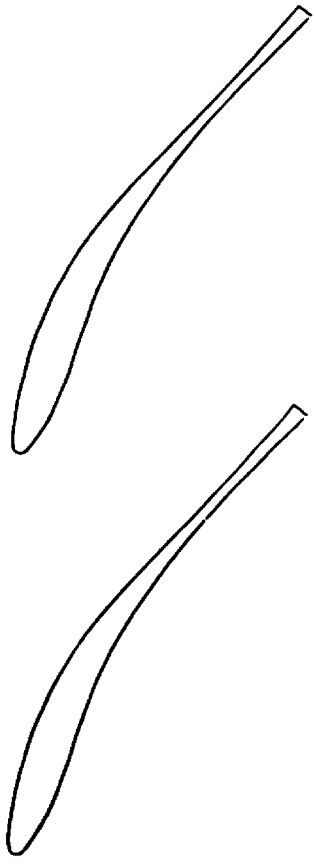

RUN	3069
RN	0.10E 07
MIN	0.259
ANIN	71.18
MEX	0.146
ANEX	51.80
TURN	19.37
SOLD	1.32
THCR	0.089
THTE	0.028
DTE	0.000

Figure 7. - High stagger subcritical rotor section.

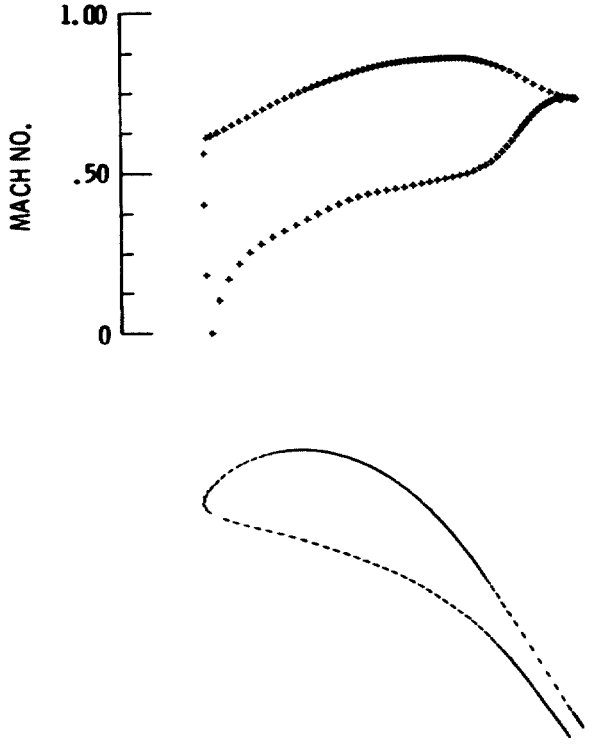

RUN	6013
MIN	0.343
ANIN	36.00
MEX	0.765
ANEX	-57.35
TURN	93.35
SOLD	1.77
THCR	0.228
THTE	0.039
DTE	-0.000

Figure 8. - Subcritical turbine blade.

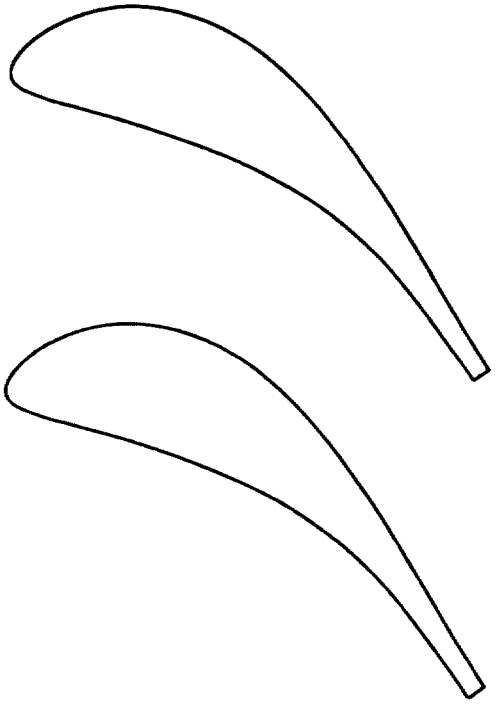

RUN	6013
RN	0.10E 07
MIN	0.343
ANIN	36.00
MEX	0.765
ANEX	-57.35
TURN	93.35
SOLD	1.77
THCR	0.228
THTE	0.033
DTE	-0.000

Figure 9. - Subcritical turbine blade.

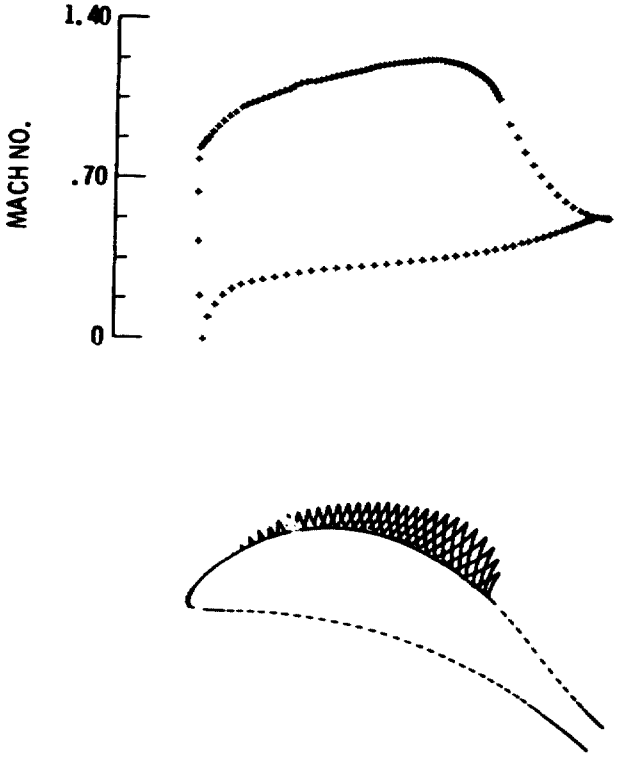

RUN	8045
MIN	0.490
ANIN	32.80
MEX	0.675
ANEX	-41.36
TURN	74.16
SOLD	0.93
THCR	0.229
THTE	0.067
DTE	-0.007

Figure 10. - Supercritical turbine blade.

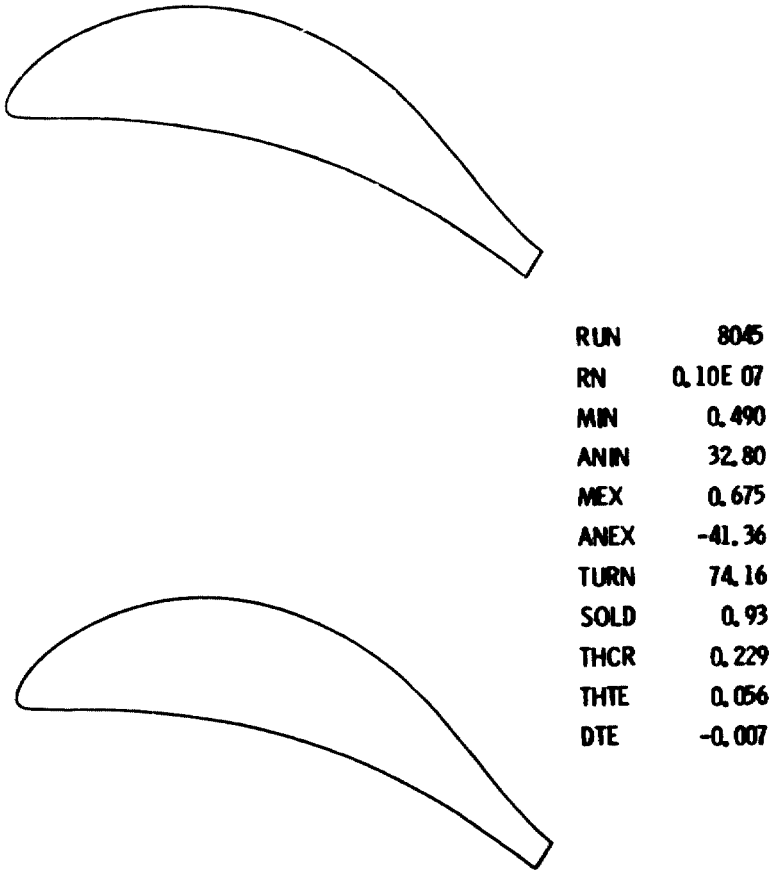

RUN	8045
RN	0.10E 07
MIN	0.490
ANIN	32.80
MEX	0.675
ANEX	-41.36
TURN	74.16
SOLD	0.93
THCR	0.229
THTE	0.056
DTE	-0.007

Figure 11. - Supercritical turbine blade.

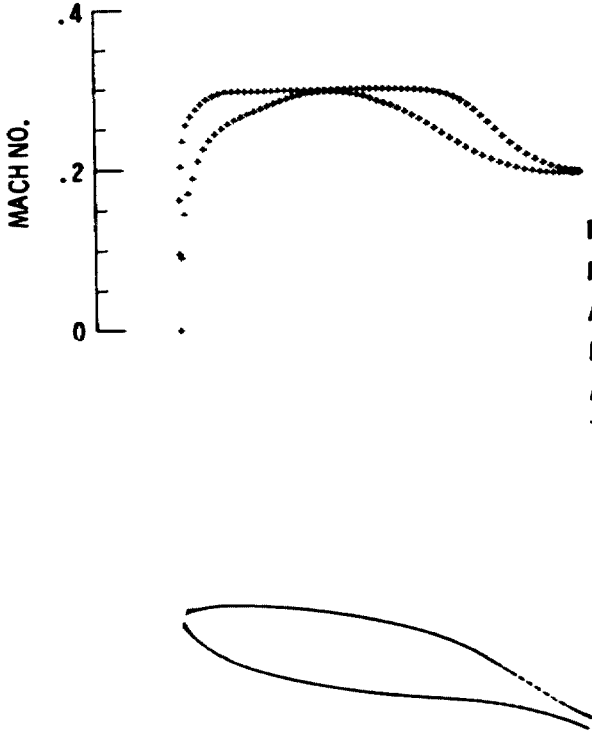

RUN	5027
MIN	0.193
ANIN	-23.94
MEX	0.208
ANEX	-25.01
TURN	1.07
SOLD	1.93
THCR	0.184
THTE	0.029
DTE	0.001

Figure 12. - Turning vane.

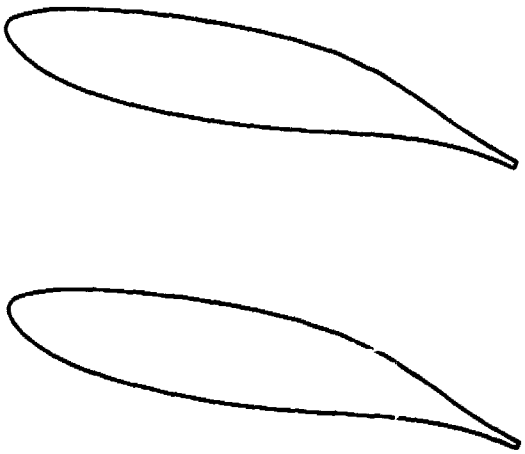

RUN	5027
RN	0.70E 07
MIN	0.193
ANIN	-23.94
MEX	0.208
ANEX	-25.01
TURN	1.07
SOLD	1.93
THCR	0.184
THTE	0.013
DTE	0.001

Figure 13. - Turning vane.

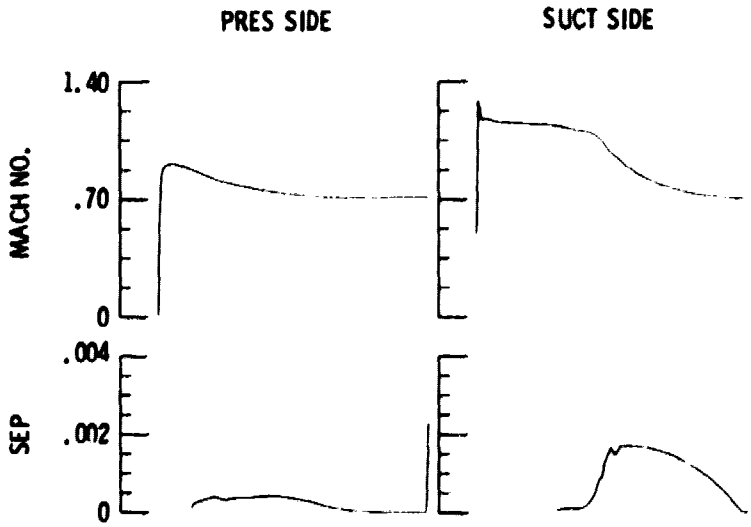

Figure 14. - Supercritical propeller section.

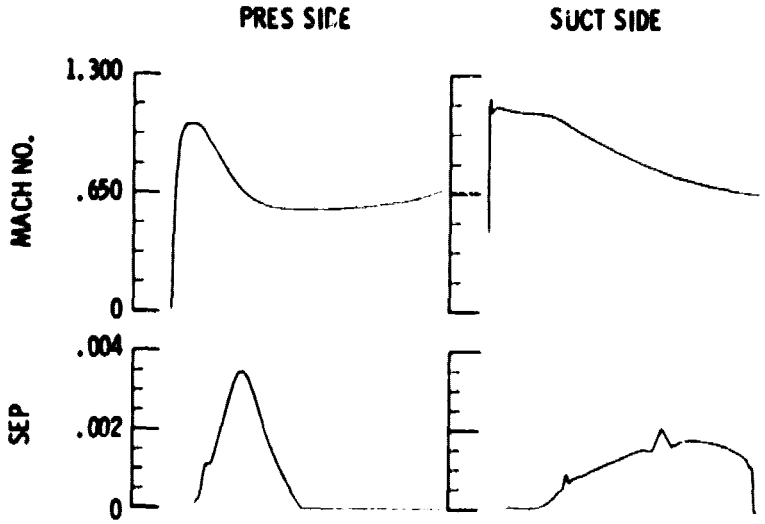

Figure 15. - Supercritical rotor section.

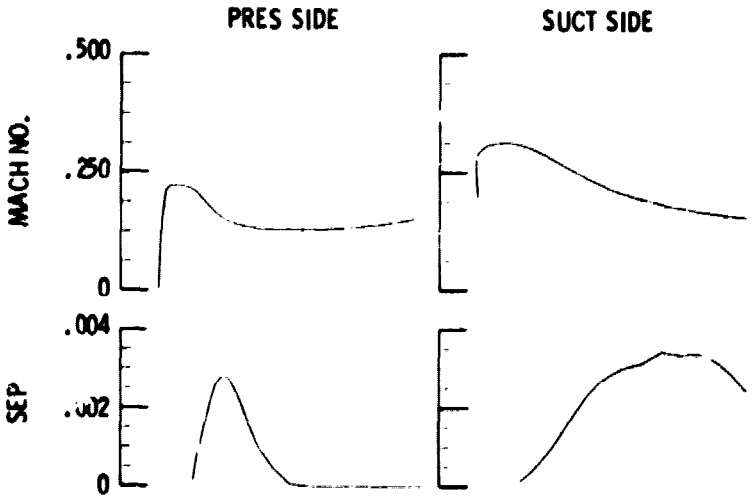

Figure 16. - High stagger subcritical rotor section.

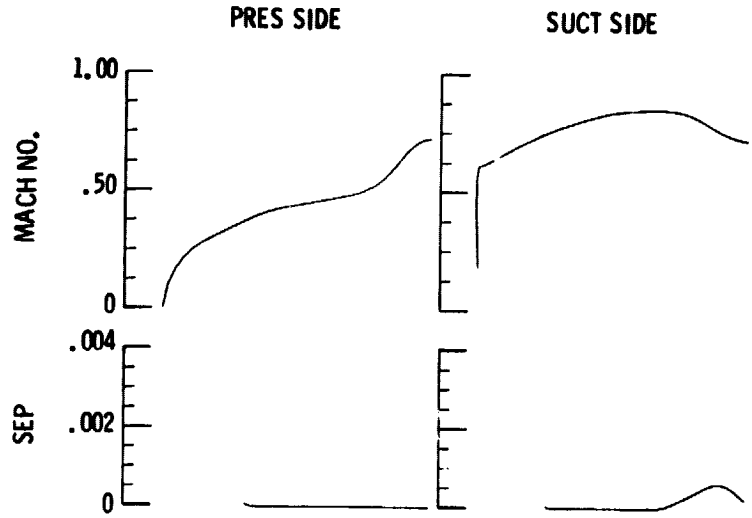

Figure 17. - Subcritical turbine blade.

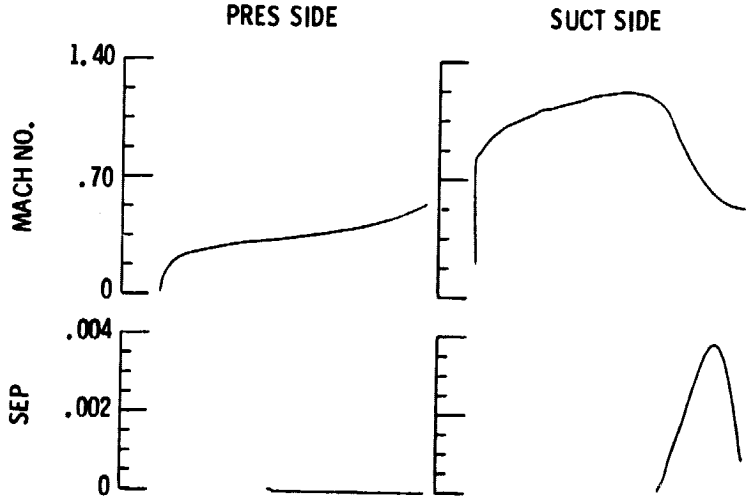

Figure 18. - Supercritical turbine blade.

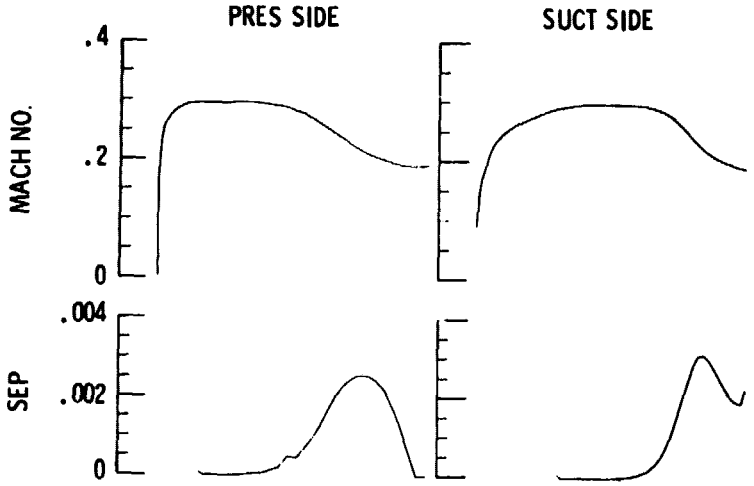

Figure 19. - Turning vane.

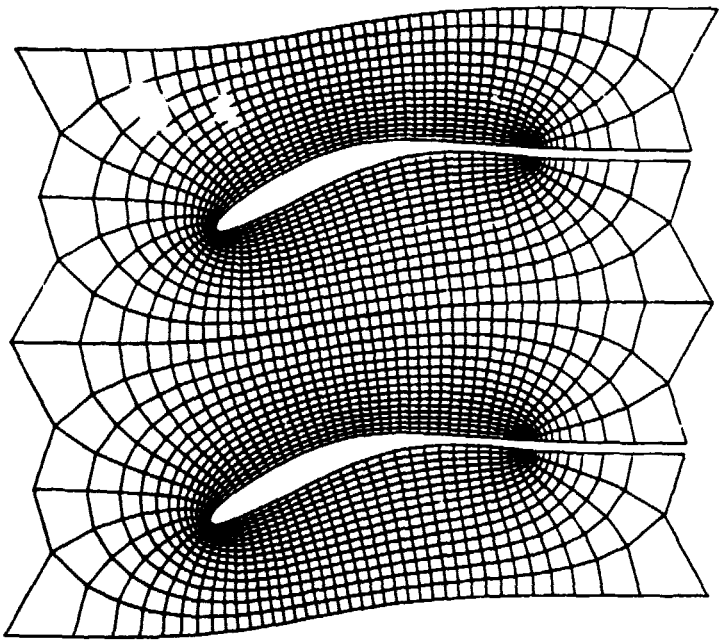

Figure 20. - Cascade grid for Korn airfoil.